Bulgarian Chemical Communications, Volume 50, Special Issue G (pp. 260 - 269) 2018

Interaction ability of metallic dibutylitin antitumor drug DPDCT with human liver isoenzyme CYP3A4 which metabolized exogenous substances

Yunlan Li[1,2*], Ying Wei[1], Xiaoqing Ji[1], Dan Wang[1], Xiaozhi Qiao[1], Qingshan Li[1,2*]

[1]*School of Pharmaceutical Science, Shanxi Medical University,Taiyuan 030001, P. R. China, Yun-lan Li:*
[2]*Shanxi University of Chinese Medicine,Key Laboratory of Innovative Drug for the Treatment of Serious Diseases Basing on the Chronic Inflammation*

Bis[2,4-dichlor-N-(hydroxy-< κ >O)benzamidato-< κ >O]diphenyltin(IV) (DPDCT), which was one of our novel patent organotin compounds with high antitumor activity and relatively low toxicity, may be the inhibitor of human CYP3A4 proteaset. In this research, DPDCT was synthesized and characterized by elemental analysis, IR, ^{1}H, ^{13}C, ^{119}Sn, NMR spectroscopic techniques, etc. The binding interaction between DPDCT and CYP3A4 was investigated by UV-vis absorption, fluorescence quenching, synchronous fluorescence, three-dimensional fluorescence, circular dichroism and molecular docking technique. The UV absorption spectra of CYP3A4 was changed with the increasing of DPDCT, the enhancement of absorption of CYP3A4 is most probably due to the formation of ground state complex from the inter-molecular interactions. The quenching rate constants and binding constants for DPDCT with CYP3A4 was determined at 298 K and 310 K, which were decreased with the increase of the temperature, showing a static quenching procedure. The apparent binding constants K_b of CYP3A4 with DPDCT at 298 K and 310 K were 3.46×10^4 and 7.59×10^3, respectively. The number of binding sit (n) were 0.87 and 1.46, respectively. The thermodynamic parameters enthalpy change (ΔH) and entropy change (ΔS) of the DPDCT -CYP3A4 complex were negative, which suggested that their interaction was mainly hydrogen bonding and van der Waals force. Gibbs free energy (ΔG) was negative, which showed the binding of DPDCT-CYP3A4 was a spontaneous process. Synchronous fluorescence and circular dichroism spectra indicated that the conformation of CYP3A4 was changed by DPDCT. The Molecular docking was used to study the interaction orientation between DPDCT and human CYP3A4 protein. The results indicated that DPDCT interacted with a panel of amino acids in the active sites of CYP3A4 protein mainly through formation of hydrogen bond. Furthermore, the predicted binding model of DPDCT into CYP3A4 appeared to adopt an orientation with interactions among Ser119.

Keywords: Dibutylitin drug DPDCT, human liver isoenzyme CYP3A4, interaction, conformational change

INTRODUCTION

Organotin (IV) compounds have received significant attentions for their potential biological activities [1]. Our research group synthesized and structurally analyzed a potential organotin candidate, bis[2,4-dichlor-N-(hydroxy-<κ>O)benzamidato<κ>O] diphenyltin(IV) (DPDCT), which exhibited the strong antitumor activity against seven human cancer cell lines including HepG-2, SHSY5Y, HEC-1-B, EC, T24, HeLa and A549 along with human liver HL-7702, a human normal hepatocytes cell [2]. In this paper, the new compound DPDCT had 2,4-dichlorophenyl groups instead of the 2,4-difluorophenyl groups of bis[2,4-difluoro-N-(hydroxy<κ>O)benzamidato<κ>O]diphenyltin(IV) (DFDPT) which had seen in the previous published paper [3]. We have designed and developed the dichloro derivative as an extension to the work previously developed with the difluoro derivative. Because DFDPT had weaker antitumor activity among our synthetic organotin compounds, we want to synthesize the more meaningful antitumor compound compared with the published DFDPT for developing a new type of potential anticancer agents, which guide us to investigate the relationship about the structure, antitumor activity and the inhibition effect on the key isoenzyme CYP3A4.

Cytochrome P450 (CYP) proteins are the most significant proteins in liver. They have many imporant physiological functions. The great anti-cancer activity of DPDCT may be relevant to the inhibition effect on the key isoenzyme CYP3A [4], which could cause the change of metabolism. A crucial fraction of the CYP family is CYP3A4, which composes up to 30% of the total liver CYP enzyme pool in humans [4-7]. The binding to CYP3A4 could affect their properties, such as absorption, distribution, metabolism, excretion, stability and toxicity. Furthermore, it has been demonstrated that the conformation of CYP3A4 will be changed upon binding with DPDCT in this paper, and the spectra change appeared to affect the secondary and tertiary structure of CYP3A4 and their biological function. The structure of DPDCT is shown in Fig.1 (a) and the structure of CYP3A4 protease is shown in Fig.1 (b), which is divided into two regions, namely α helix and β fold region.

* To whom all correspondence should be sent:
liyunlanrr@163.com

© 2018 Bulgarian Academy of Sciences, Union of Chemists in Bulgaria

Heme is the binding site of oxygen and substrate in the oxidation reaction. Central iron atom of heme is the non-covalent binding form in the CYP3A4 molecule.

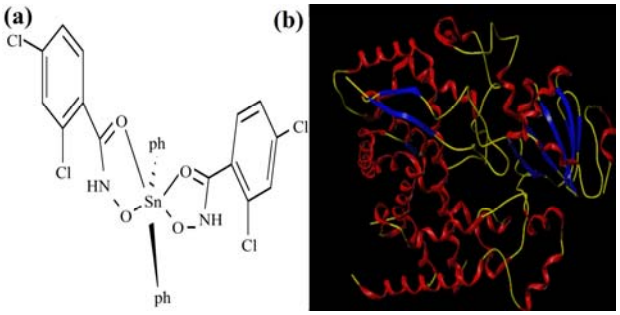

Fig.1. Structure of DPDCT and CYP3A4 protease. (a) DPDCT (b) CYP3A4 protease

Up to now, many methods have been used for the investigate the complex-protein interaction, such as NMR, UV-Vis spectrophotometry, FT-IR, fluorescence, CD and molecular docking and so on [8-12]. Among these methods, fluorescence spectroscopy has a variety of superior advantages over other techniques because of its high sensitivity, rapidity and ease of implementation. Fluorescence spectroscopy is an effective method to reveal the interaction between small molecules and proteins [13]. In this paper, we have studied the interaction of DPDCT with CYP3A4 protein by the fluorescence quenching method. The binding constants were obtained at different temperatures in the medium of PBS (pH 7.4) buffer solution. The binding site and main sorts of binding forces have been suggested. In addition, the conformational changes of CYP3A4 protein were discussed on the basis of UV-visible spectroscopy, synchronous fluorescence (SF), CD and three-dimensional spectroscopy[14-17]. Molecular docking can be used to study the metabolic behavior of the compounds through docking the compounds into the activity sites of drug-metabolizing enzymes. In addition, understanding the interaction of DPDCT with CYP3A4 protein could contribute to the clinical employment of the organotin compounds and the relief of the organotin pollutant. Therefore, the aim of the present study is to determine the binding of DPDCT towards the activity cavity of CYP3A4 protein. Through these data, it may help us find more particular information regarding their metabolism in the human body, and give us a better understanding for its biological action [18,19].

EXPERIMENTAL

Synthesis of DPDCT

Di-phenyltin dichloride (0.344 g, 1.0 mmol) was added to an anhydrous methanol solution (20 mL) of 2, 4–di-chlorbenzohydroxamic acid (0.412 g, 2.0 mmol) and potassium hydroxide (0.112 g, 2.0 mmol). The solution was stirred at room temperature per overnight. Water (20 mL) was added and a white precipitate was formed. Then filtrate and vacuum dry. Yield: 82%; m.p.133-135oC. Calcd (%) for C26H18N2O4Cl4Sn : C, 45.68 ; H, 2.64 ; N, 4.10. Found (%) : C, 45.52 ; H, 2.90 ; N, 4.01. IR : ν= (N–H) 3211 (s), ν= (CO/NC) 1593(s), 1520(w), (N–O) 919 (s), (Sn–C) 557 (m), (Sn–O) 523 (m), 448(s) cm-1. 1H NMR（CDCl3）: δ= 10.08 (s, br,2H, NH), 7.98 ~ 7.15 (m, 16H, Harom) ppm. 13C NMR (CD3OD) : δ= 175.8 (CO); 161.1, 150.4, 134.5-126.8, 110.5, 105.7 (Carom) ppm. 119Sn NMR (CDCl3) : δ= −339.8,-427.1 ppm. ESI-MS, m/z = 681.9 [M]+.

UV-vis absorption studies

The UV-vis absorption spectra can be usually used to determine the structural change of biomacromolecules. The results from UV-vis absorption spectra are usually in agreement with CD measurements which are useful tools to study the interaction conformation. The concentration of CYP3A4 was constant (5×10^{-9} mol·L^{-1}) while varying the compound DPDCT concentration (0, 0.5×10^{-5}, 1×10^{-5}, 1.5×10^{-5}, 2×10^{-5}, 2.5×10^{-5}, 3×10^{-5}, 3.5×10^{-5} and 4×10^{-5} mol·L^{-1}). We measured scan curves in the range of 280 nm to 350 nm at 310K.

Fluorescence quenching spectra

The emission wavelength was performed from 300 nm to 400 nm. The excitation wavelength was at 280 nm. The concentration of CYP3A4 was constant (5×10^{-9} mol • L^{-1}) while varying the compound DPDCT concentration (0, 0.5×10^{-5}, 1×10^{-5}, 1.5×10^{-5}, 2×10^{-5}, 2.5×10^{-5}, 3×10^{-5}, 3.5×10^{-5} and 4×10^{-5} mol • L^{-1}). The excitation and emission band widths were 5nm. Fluorescence spectra were recorded (n = 3 replicates) on LS-55 fluorophotometer (Perkin Elmer, USA) equipped with a 150 W Xenon lamp , a HH-2 waterbath (Changzhou Guohua Electric Applance Co. Ltd, Changzhou, China) and 1.0 cm quartz cells. Then we measured fluorescence quenching spectra.

Synchronous fluorescence

In order to investigate the structural change of CYP3A4 in the presence of DPDCT, we measured synchronous fluorescence spectra of CYP3A4. In this method, Δλ stands for the value of the difference between excitation and emission wavelengths. When Δλ is 15 nm or 60 nm, the synchronous fluorescence spectroscopy just shows the spectroscopic behavior of Tyr residue or Trp residue of proteins, separately. Therefore, synchronous fluorescence spectra of CYP3A4 (1×10^{-8}mol·L^{-1}) with complex DPDCT (0, 0.5×10^{-5}, 1×10^{-5}, 1.5×10^{-5}, 2×10^{-5}, 2.5×10^{-5}, 3×10^{-5}, 3.5×10^{-5} and 4×10^{-5} mol·L^{-1}, respectively) at Δλ = 15 nm and Δλ = 60 nm were recorded on LS-55 fluorescence spectrophotometer.

Energy transfer

Fluorescence resonance energy transfer (FRET) is a reliable method for studying protein-ligand interaction and evaluation of the distance between the ligand and tryptophan residues of the protein. In the method, the absorption spectrum of DPDCT(5×10^{-9} mol • L^{-1}) was recorded in the range of 300-500 nm.Then, the overlap of the UV h the absorption spectrum of DPDCT with the fluorescence emission spectrum of CYP3A4(5×10^{-9} mol • L^{-1}) was uesd to calculate the energy transfer.

Three-dimensional fluorescence

It is well known that three-dimensional fluorescence can provide more detailed information about the conformational changes of proteins. The maximum emission wavelength and the fluorescence intensity of the residues have a close relation to the polarity of their micro-environment. By comparing the three-dimensional fluorescence spectral changes of CYP3A4 protein in the absence and presence of DPDCT, we can investigate the conformational and micro-environmental changes of CYP3A4. In this research, the three-dimensional fluorescence spectroscopies of CYP3A4 protein (5×10^{-9} mol • L^{-1}) treated with DPDCT (0 and 3×10^{-5} mol • L^{-1}) were measured on F-320 fluorophotometer (Tianjin Gangdong Sci. &Tech. Development Co. Ltd., Tianjin, China). The emission wavelength was recorded between 320 nm and 450 nm with an increment of 10 nm. The excitation wavelength was performed between 200 and 300 nm with an increment of 10 nm. The photomultiplier tubes（PMT）voltage was set at 700 V. The scan speed was set at 12000 nm/min.

CD measurements

CD is a powerful tool in elucidating the modifications of the secondary structure of biopolymers as a result of interaction with small molecules. CD measurements were recorded on a MOS - 450 spectropolarimeter at room temperature under constant nitrogen flush. Quartz cells have pathlength and volume of 0.1 cm and 400 μl, respectively. The acquisition duration was 0.5 s and the scan step was 1 nm in the range of 200-250 nm of scan repeat 3 times. The CD measurements of CYP3A4 constant (5×10^{-9} mol • L^{-1}) in the absence and presence of the varying DPDCT concentration (0, 1×10^{-5}, 2×10^{-5} and 3×10^{-5} mol • L^{-1}). Appropriate blank ran under the same conditions, it was subtracted from the sample spectra.

Molecular docking

The structure of cytochrome P450 CYP3A4 was obtained from Protein Data Bank (http://www.rcsb.org/pdb) and PDB code was 4K9W. The two-dimensional structure of DPDCT with standard bond lengths and angles was drawn using Sybyl-X 2.0. The chains of B, C and D of 4K9W were eliminated. Minimization of molecular energy was carried out with the Tripos force field. The most stable conformation was searched using the Powell conjugate gradient algorithm with a convergence criterion of 0.001 kcal/mol. The limit of energy gradient was 0.05 kcal/mol Å. The compound partial charges were calculated using Gasteiger-Huckel method. CYP3A4 was carried out with the AMBER 7FF99 force field. The protein partial charges were calculated using AMBER method. The docking process was performed with Surflex-Dock (within Sybyl-X 2.0, Tripos international). Docking of ligands into the catalytic domain of the CYP3A4 model was carried out using Surflex-Dock. The top 20 ranked ligands are flexible compounds that can adopt a multitude of conformations within the CYP3A4 active site.

RESULTS AND DISCUSSIONS

Structure characterization

Comparing with the free ligand of the FT-IR spectra, the broad band O-H absorption of 2479 cm^{-1} was absent, because of the deprotonation and coordination. The absorption band of C=O from

1598 cm^{-1} and 1562 cm^{-1} in the free ligand to 1593cm^{-1} and 1520 cm^{-1} indicated this group occurred coordination. The absorption band of N-O was 901cm^{-1} in the free ligand and 919cm^{-1} in the complex. In the complex, the Sn-C absorption was exhibited 557 cm^{-1}, the Sn-O absorption were exhibited 523cm^{-1} and 448 cm^{-1}. In the ^{1}H NMR spectrum, DPDCT showed the expected resonances. It exhibited resonances in the range of 7.98-7.15 ppm. 13C NMR spectrum exhibited the C=O signal around the tin atom and the phenyl carbon signal. 119Sn NMR spectra showed the same-type organotin resonance at –339.8 and –427.1 ppm.

UV-Vis spectral measurements

The UV-Vis absorption spectra of CYP3A4 in the presence of increasing concentration of DPDCT (0, 0.5×10^{-5}, 1×10^{-5}, 1.5×10^{-5}, 2×10^{-5}, 2.5×10^{-5}, 3×10^{-5}, 3.5×10^{-5} and 4×10^{-5} mol • L^{-1}) are measured at stimulated physiological condition. In presence of increasing concentration of DPDCT, the absorption spectra of pure CYP3A4 gradually increases. Fig.2. shows the absorption spectra of CYP3A4 and CYP3A4 in the presence of increasing concentration of DPDCT.

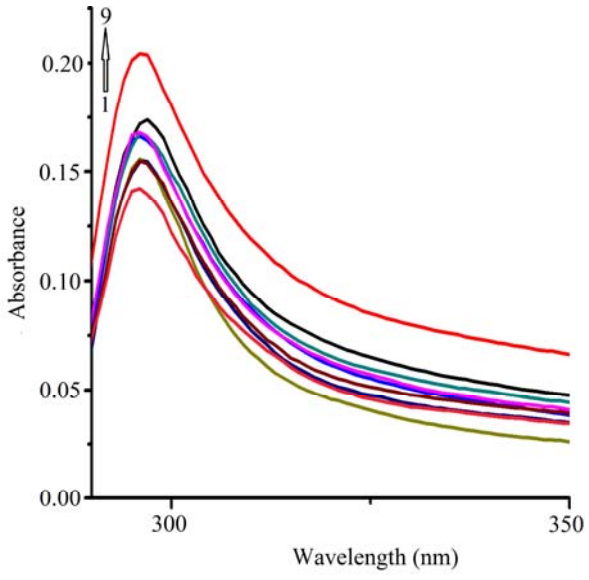

Fig.2. UV-vis spectra of CYP3A4 protein (5×10^{-9} mol·L^{-1}) in the absence and in the presence of increasing DPDCT concentrations in pH 7.4 PBS buffer. From 1 to 9 lines, concentrations of DPDCT were: 0, 0.5×10^{-5}, 1×10^{-5}, 1.5×10^{-5}, 2×10^{-5}, 2.5×10^{-5}, 3×10^{-5}, $3.5\times10^{-5}$and 4×10^{-5} mol·L^{-1}, respectively.

From the Fig.2, it can be observed that the intensity increases significantly as the quencher concentration increased. The increase in intensity can be attributed to the formation of the ground state complex between CYP3A4 protein and DPDCT, as CYP3A4 molecules get absorbed on the surface of DPDCT. As the concentration of DPDCT used possesses negligible absorbance in the region of absorption spectra of CYP3A4, the enhancement of absorption of CYP3A4 is most probably due to the formation of ground state complex from the inter-molecular interactions [20].

Fluorescence quenching results

1. The value of quenching constant

As is well known, the intrinsic fluorescence of CYP3A4, which comes from tryptophan (Trp), tyrosine (Tyr) and phenylalanine (Phe) residues, is often used to be an endogenous fluorescent probe to study the conformational change of CYP3A4 in the binding process of CYP3A4 with compounds. However, Trp residue has the strongest fluorescence intensity and is the most sensitive to the changes in the micro-environment. The fluorescence quenching of protein can be divided into three quenching mechanisms. The static quenching caused by forming ground-state complex of protein with quenchers, the dynamic quenching caused by the collsion of protein and quenchers, and combined dynamic and static quenching caused both collision and complex formation with the same quencher, respectively. In the case of the static quenching, the value of quenching constant (Ksv) decreased with the increase of temperature due to higher temperature resulting in the decrease of the complex stability. In contrast, for the dynamic quenching process, the value of Ksv increased with the increase of temperature due to higher temperature resulting in larger diffusion coefficient and promotes electron transfer [21,22]. In order to research the binding of CYP3A4 protein to DPDCT, the fluorescence spectra were recorded from 300 nm to 400 nm upon excitation at 280 nm. Fig.3. showed the fluorescence spectrum of CYP3A4 in the absence and presence of different DPDCT concentrations at 298 K and 310 K. The fluorescent intensity of CYP3A4 protein decreased regularly with increasing concentration of DPDCT, while the maximum emission wavelength was almost not changed, suggested that a change in the surrounding environment of the fluorophores due to binding interaction with DPDCT and the binding region of DPDCT is the vicinity of Trp residues

since a distant event cannot cause its fluorescence quenching.

The fluorescence quenching data were analyzed by the well-known Sterne-Volmer equation [23,24]:

$$\frac{F_0}{F} = 1 + K_{SV}[Q] = 1 + K_q \tau_0 [Q] \quad (1)$$

where, F_0 and F are the fluorescence emission intensities in the absence and presence of quencher, respectively; K_q is the quenching rate constant, Ksv is the Stern–Volmer quenching constant which measures the efficiency of quenching; [Q] is the concentration of the DPDCT, τ_0 is the average lifetime of fluorophore in the absence of quencher and its value is considered to be fluorophore 10^{-8} s. The Stern–Volmer equation was applied to determine Ksv by linear of a plot of F_0/F versus [Q]. The Stern-Volmer plots of the quenching of CYP3A4 protein fluorescence quenched by DPDCT at different temperatures were shown in Fig.4 (a) and (b). The Stern-Volmer quenching constants K_{sv} and K_q at different temperatures were obtained and listed in Tab.1.

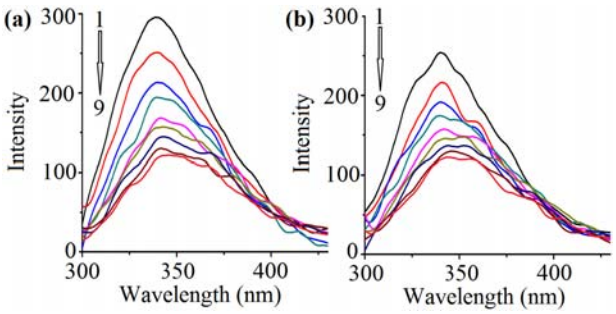

Fig.3. Fluorescence emission spectra of CYP3A4 protein(5×10^{-9}mol·L^{-1}) in the absence and in the presence of increasing DPDCT concentrations in pH 7.4 PBS buffer. (a). T = 298 K. (b). T = 310 K. From 1 to 9 lines, concentrations of DPDCT were: 0, 0.5×10^{-5}, 1×10^{-5}, 1.5×10^{-5}, 2×10^{-5}, 2.5×10^{-5}, 3×10^{-5}, 3.5×10^{-5} and 4×10^{-5} mol·L^{-1}, respectively. λ_{ex} = 280 nm.

Table 1. Quenching constants of CYP3A4 protein with DPDCT at different temperatures

T (K)	K_{SV} (L mol^{-1})	K_q (L mol^{-1} s^{-1})	R^2
298	3.56×10^4	3.56×10^{12}	0.996
310	2.59×10^4	2.59×10^{12}	0.995

A plot of (F_0/F) versus [Q] yields straight line in case of single fluorophore. The plots showed good linear relationships within the investigated concentrations (R^2 = 0.996 at 298 K and R^2 = 0.995 at 310 K). Linear fittings of the experimental data obtained afford K_{sv} and K_q. K_sv is the 3.56×10^4 L mol^{-1} at 298 K and the 2.59 $\times10^4$ L mol^{-1} at 310 K. Tab.1 shows that K_{sv} values were inversely correlated with temperatures, which suggested that the fluorescence quenching of CYP3A4 was initiated by the formation of ground-state complex. For dynamic quenching, the maximum scattering collision quenching constant of various quenchers is 2.0×10^{10} L mol^{-1} s^{-1} .The results showed that the value of K_q was much greater than 2.0×10^{10} which indicated that the probable quenching mechanism of fluorescence of CYP3A4 by DPDCT is not caused by dynamic collision but from the formation of a complex.

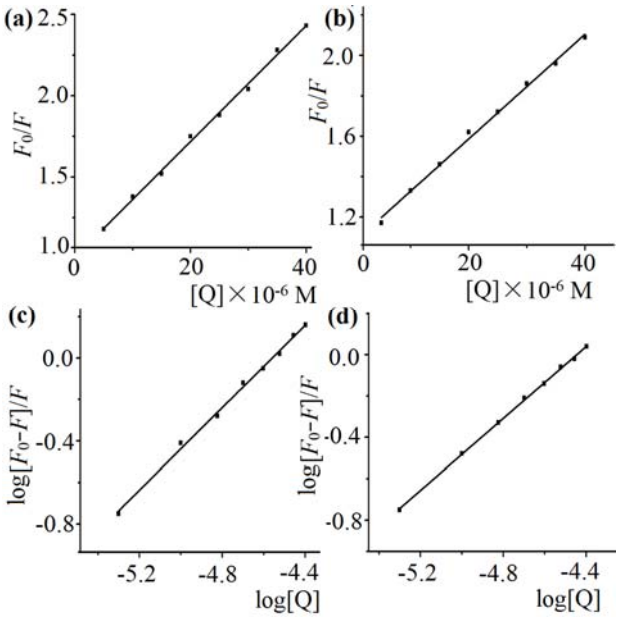

Fig.4. Stern–Volmer plots of CYP3A4 protein (5×10^{-9} mol • L^{-1}) quenched by DPDCT at different temperatures. (a). T = 298 K. (b). T = 310 K. A plot of log[(F_0-F) / F] vs log [Q] of DPDCT with CYP3A4 protein (5×10^{-9} mol • L^{-1}) at different temperatures. (c). T = 298 K. (d). T = 310 K. λ_{ex} = 280 nm

2. Binding constants and binding sites

When small molecules bind independently to a set of equivalent sites on a macromolecule, the equilibrium between free and bound molecules is given by the following equation [25]:

$$\log\frac{F_0 - F}{F} = \log K_b + n\log[Q] \quad (2)$$

where K_b and n are the binding constant and the number of binding sites, respectively. Thus, the K_b and n values can be obtained from the intercept and slope values of the plot of log $[(F_0\text{-}F)/F]$ against log$[Q]$ as in Fig.4.(c) and (d). The plots showed good linear relationships within the investigated concentrations (R^2 = 0.9900 at 298 K and R^2 = 0.9990 at 310 K). The values of K_b and n for the DPDCT-CYP3A4 system at 298K were estimated to be 3.46×10^4 and 0.99. The values of K_b and n for theD PDCT-CYP3A4 system at 310K were estimated to be 7.59×10^3 and 0.87, respectively. The values of n are roughly equal to 1.

Table 2. The binding constants and the number of binding sites of CYP3A4 protein with DPDCT at two different temperatures

T (K)	K_b (L mol^{-1})	n	R^2
298	3.46×10^4	0.99	0.9900
310	7.59×10^3	0.87	0.9990

Tab.2 gives the corresponding calculated results.The results showed that Kb were decreased with the increasing temperature, which may hint the formation of an unstable complex in the binding reaction. The complex would be partly decomposed with the increasing temperature, therefore, the K_b decreased. Furthermore, the values of n were approximately equal to 1, manifesting the existence of just a single binding site in CYP3A4 protein towards DPDCT. The previous compound DFDPT which has the 2,4-difluorophenyl groups had the apparent binding constants K_b of CYP3A4 at 298 K and 310 K of 2.51×10^7 and 3.09×10^5. So the diversity of substituent 2,4-dichlorophenyl groups instead of the 2,4-difluorophenyl groups of bis [2,4-difluoro-N-(hydroxy-< κ >O)benzamidato-< κ >O]diphenyltin(IV) shows the strong discrepancy in the binding intensity. The fluorinated group of DFDPT has the impressive interaction with CYP3A4 than the chlorinated group of the organotin antitumor compound DPDCT.

Thermodynamic analysis of binding mode

There are mainly four types of noncovalent interactions that could play a role in ligand binding to proteins. They are hydrogen bonds, van der Waals forces, electrostatic, and hydrophobicinter-actions, respectively. The model of interaction can be summarized as : (1) $\Delta H > 0$ and $\Delta S > 0$, hydrophobic forces; (2) $\Delta H < 0$ and $\Delta S < 0$, van der Waals interactions and hydrogen bonds; (3) $\Delta H < 0$ and $\Delta S > 0$, electrostatic interaction. The thermodynamic parameters including ΔH，ΔS and ΔG can be calculated from the Van't Hoffequation :

$$\Delta G=-RT\ln K \quad (3)$$

$$\ln\frac{K_2}{K_1}=(\frac{1}{T_1}-\frac{1}{T_2})\frac{\Delta H}{R} \quad (4)$$

$$\Delta S=\frac{\Delta H-\Delta G}{T} \quad (5)$$

Where K_1 and K_2 are the binding constants at corresponding temperature (T_1 and T_2), and R is the gas constant. The temperatures used were 298 and 310 K. ΔH, ΔS and ΔG are enthalpy change, entropy change and free energy change, respectively. The free energy change ΔG is estimated from the Eq. (5). Tab.3 shows the values of ΔH and ΔS obtained for the binding site from the slopes and ordinates at the linear Van't Hoff .

Table 3. Thermodynamic parameters of the interaction between DPDCT and CYP3A4

T (K)	ΔH（kJ mol^{-1} ）	ΔS（J K^{-1} ）	ΔG（kJ mol^{-1} ）
298	-97.01	-238.66	-25.89
310	-97.01	-238.65	-23.03

From Tab.3, it can be seen that the negative sign for free energy ΔG means that the interaction process is spontaneous. $\Delta H < 0$ indicated the formation of DPDCT-CYP3A4 coordination was exothermic. Therefore, both ΔH and ΔS are negative value indicated that both hydrogen bond and van der Waals forces play the major role in the interaction of DPDCT and CYP3A4 protein.

Characteristicsof synchronous fluorescence spectra

Unlike the steady-state fluorescence spectra, synchronous fluorescence spectroscopy can provide the characteristic information about the microenvironment in a vicintity of disparate chromophores. When setting the scanning intervals ($\Delta\lambda = \lambda_{emi} - \lambda_{exc}$) of 15 and 60 nm, the characteristic information of the Tyr and Trp residues can be obtained. The research results had demonstrated that the shift of the maximum emission wavelength represents the alteration of the polarity of the microenvironment surrounding Tyr or Trp residues and the red shift of the maximum emission wavelength indicates that the hydrophobicity surrounding Tyr or Trp residue decreases and the stretching extent of the peptide chain increases [26]. The effect of DPDCT on the synchronous fluorescence spectrum of CYP3A4 protein was showed in Fig.5. Analysizing the Fig.5 (a), the tyrosine residues fluorescence emission was

blue-shift, it demonstated the microenvironment of the tyrosine residues had been changed in the direction of increasing the hydrophobicity of the microenvironment. From Fig.5 (b), it was observed that the maximum emission wavelength of the tryptophan residues was red-shifted with the increasing concentration of DPDCT. It demonstated the microenvironment of the tryptophan residues had been changed in the direction of reducing the hydrophobicity of the microenvironment.

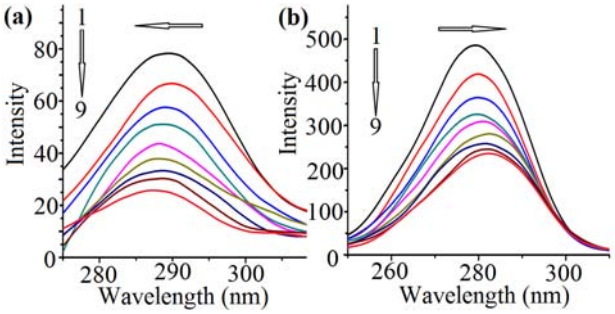

Fig.5. Synchronous fluorescence spectra of CYP3A4 protein (1×10^{-8} mol·L^{-1}) in the absence and presence of DPDCT. A. the wavelength difference $\Delta\lambda$ =15 nm B. the wavelength difference $\Delta\lambda$ = 60 nm. [DPDCT] 1→9: 0, 0.5×10^{-5}, 1×10^{-5}, 1.5×10^{-5}, 2×10^{-5}, 2.5×10^{-5}, 3×10^{-5}, 3.5×10^{-5} and 4×10^{-5} mol·L^{-1}, respectively.

Energy transfer

According to Forster non-radioactive energy transfer theory, the energy transfer will happen under the following conditions: (a) the donor can produce fluorescence light, (b) there is significant overlap between fleorescence emission spectrum of the donor and UV absorption spectrum of the acceptor and (c) the distance between the donor and the acceptor is lower than 8nm. The fluorescence spectrum of CYP3A4 ans the absorption spectrum of DPDCT is shown in Fig.6. The energy transfer efficiency E is defined by the following equation:

$$E = \frac{R_0^6}{(R_0^6 + r^6)} = 1 - \frac{F}{F_0}$$

where r is the distance between the acceptor and the donor, and R_0 is the Forster critical distance, at which 50% of the excitation energy is transferred to the acceptor. F and F_0 are the fluorescence intensities of CYP3A4 in the presence and absence of DPDCT. R_0 can be calculated from donor emission and acceptor absorption spectra using the Forster formula, that is the following equation:

$$R_0 = 8.8\times10^{-25}k^2N^{-4}\Phi J$$

where k_2 is the spatial orientation factor of the dipole (k_2=2/3); N, the refractive index of the medium (N=1.336); Φ, the fluorescence quantum yield of the donor (Φ=0.118); and J is the overlap integral of the fluorescence emission spectrum of the donor and the absorption spectrum of the acceptor J is given by:

$$J = \sum F(\lambda)\varepsilon(\lambda)\lambda^4 \Delta\lambda / \sum F(\lambda)\Delta\lambda$$

where $F(\lambda)$ is the fluorescence intensity of the fluorescent donor of wavelength λ; $\varepsilon(\lambda)$ and is the molar absorption coefficient of the acceptor at waclength λ. We have obtianed that $J=9.43\times10^{-20}$ cm^6 Lmol^{-1}, $R_0^6= 2.60\times10^{-45}$ cm^6, the energy can transfer from CYP3A4 to DPDCT with high probability and the distance obtained by FRET with higher accuracy.

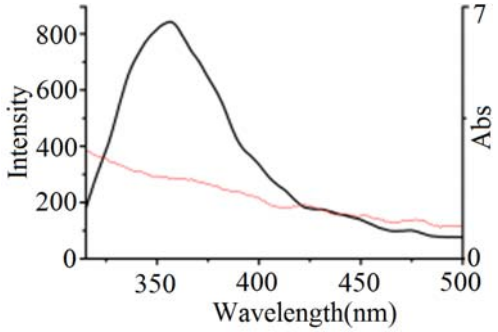

Fig.6. The fluorescence spectrum of CYP3A4 and the absorption spectrum of DPDCT

3D fluorescence spectroscopy

Three-dimensional (3D) fluorescence spectroscopy has become a popular fluorescence analysis technique in recent years. It is well known that three-dimensional fluorescence spectrum can provide more detailed information about the change of the configuration of proteins. By comparing the 3D fluorescence spectroscopy changes of CYP3A4 protein in the absence and presence of DPDCT, we can investigate the conformational and micro-environmental changes of CYP3A4. The contour maps of CYP3A4 and CYP3A4-DPDCT system were shown in Fig.7 and Table 4. In Fig.7, peak A (λ_{ex}=230nm, λ_{em}=320nm) exhibited the fluorescence characteristic of polypeptide backbone structures, and Peak B (λ_{ex}=280 nm, λ_{em}=330nm) was the characteristic spectroscopy of tryptophan and

tyrosine residues. Fig.7 presents the contour maps of CYP3A4 and DPDCT–CYP3A4.

Table 4. The characteristic parameters of three dimensional fluorescence spectra of CYP3A4 and CYP3A4-DPDCT system

Fluorescence peak A		Fluorescence peak B	
Peak position $\lambda_{ex}/\lambda_{em}$ (nm/nm)	Intensity F	Peak position $\lambda_{ex}/\lambda_{em}$ (nm/nm)	Intensity F
230/325.0	218.2	280/331.8	2040.8
230/329.6	116.4	280/332.4	1466.4

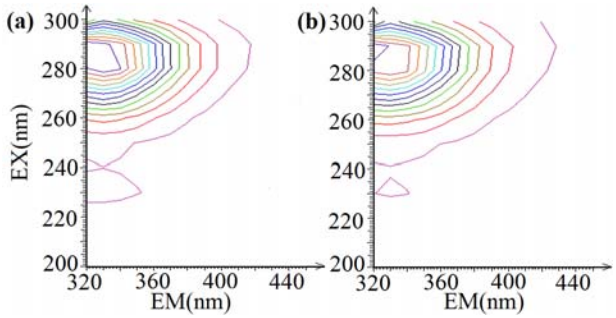

Fig.7. Three-dimensional fluorescence contour maps of CYP3A4 and CYP3A4 - DPDCT system. (a). CYP3A4 (5×10^{-9}mol·L^{-1}) (b). CYP3A4-DPDCT （DPDCT: 3×10^{-5} mol·L^{-1}）

From Tab.4, we found the intensity of peak A was decreased and the emission wavelength was shifted, which implied that the peptide strand structure of CYP3A4 was changed. And, the intensity of peak B was decreased and the emission wavelength was shifted, which demonstrated that the microenvironment of Trp and Tyr residues had been changed. The decrease of the intensity of the peak A and peak B in combination with the fluorescence emission spectra indicated that the binding of DPDCT with CYP3A4 causes slight unfolding of the polypeptide chain of CYP3A4 and conformational change of CYP3A4. This suggests that the bindingof DPDCT–CYP3A4 induced some microenvironmental and conformational changes in CYP3A4, and a complex between them may has been formed [27].

Circular dichroism spectroscope

The CD spectra of CYP3A4 protein in the absence and presence of DPDCT were shown in Fig.8.

The results revealed that there was a band at near 220 nm, which exhibited a typical shape of α-helix secondary structure. The intensities of band slightly decreased with the addition of DPDCT along with the slightly blue shift of the peak at near 220 nm, which indicating that the CYP3A4 still retained its secondary α-helix structure and α-helix content of CYP3A4 was decreased after DPDCT binding to CYP3A4.

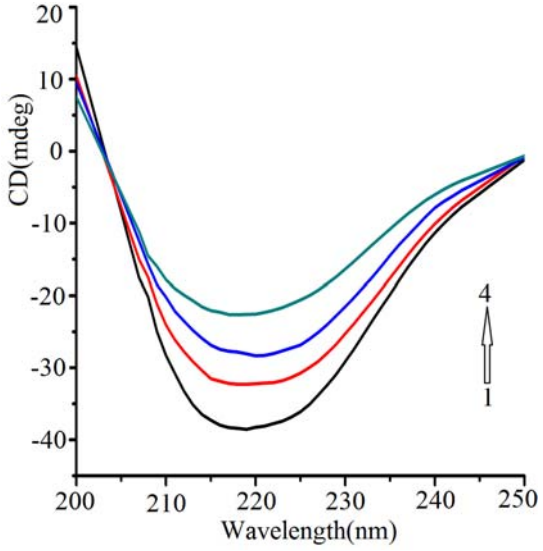

Fig.8. Circular dichroism of CYP3A4 protein (5×10^{-9} mol·L^{-1}) and DPDCT in PBS buffer (pH 7.4, from 1→4, concentrations of DPDCT were: 0, 1×10^{-5}, 2×10^{-5} and 3×10^{-5} mol·L^{-1}, respectively)

Molecular docking

In the field of molecular modeling, molecular docking is a useful method which predicted the preferred orientation of a small molecule to biomacromolecule when bound to each other to form a stable complex and the strength of association between molecules using scorning functions. The molecular docking technique is a fascinating method to study the interaction between drugs and CYP3A4 The binding orientation of DPDCT on CYP3A4 protein were shown in Fig.9(a) which indicated that DPDCT binded to CYP3A4 internal structure. In the Fig.9(b), red link represented the connection bonds of oxygen atom, and blue link represented the connection bonds of nitrogen atom. From our docking results, DPDCT might bind Ser119 of CYP3A4, which thus affects the combination of DPDCT and CYP3A4. DPDCT enters into the cavity of CYP3A4 via hydrogen bonds. There are hydrogen bonds between DPDCT and residues Ser119 (distance, 2.53 and 2.26 Å). The next step, we want to use the CYP3A4 mutant to verify the connection bonds by a variety of spectroscope techniques.

Compared with the previous compound which has the 2,4-difluorophenyl groups, DPDCT enters into the cavity of CYP3A4 through one hydrogen bonding (Ser119). But the previous compound

connected the cavity of CYP3A4 by three hydrogen bonding (Arg105, Ser119 and Thr309). It testified DPDCT had the weaker binding constants.

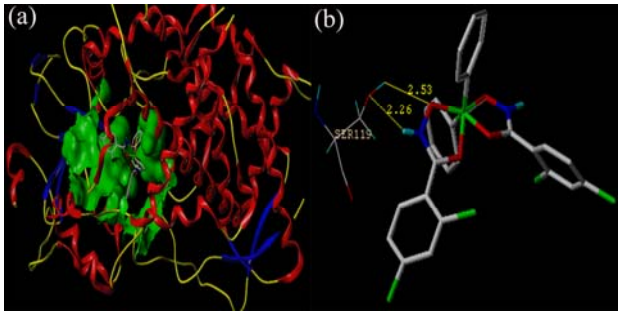

Fig.9. The docking of DPDCT into the activity of CYP3A4 protein. (a). The binding orientation of DPDCT with CYP3A4 (b).Structural details of the interaction between DPDCT and CYP3A4.

CONCLUSIONS

Compared with the published DFDPT, the DPDCT is the more meaningful antitumor compound. The IC_{50} value of DPDCT against human HEC-1-B cell lines was 5.12 μmol·L^{-1}, while the IC_{50} values of the DFDPT was 12.30 μmol·L^{-1} by MTT assay according to the standard procedures. In the human SHSY-5Ycell lines, the IC_{50} values of DPDCT is 8.20 μmol·L_{-1}, while the DFDPT has the antitumor activity of IC_{50} values of 12.88 μmol·L^{-1}. In the human T24、HepG-2 and Hela cells, the new compound DPDCT also had higher antitumor activity than the published DFDPT. The DPDCT is the higher-activity compound which lay the foundation for further design and structure optimization to synthesis the more impressive antitumor activity compound. In this work, we used different approaches to explore the interactions between DPDCT and CYP3A4 under physiological conditions. The experimental results showed that DPDCT quenches the fluorescence of CYP3A4 by a static quenching mechanism. Experimental results from the quantitative analysis of circular dichroism, three dimensional fluorescence studies and synchronous fluorescence spectrum demonstrated that the binding of DPDCT to CYP3A4 protein induced some micro-environmental and conformational change of CYP3A4. Our study is expected to provide important protein into the interaction of the physiologically protein with DPDCT, facilitating further investigation on the pharmacological behavior of DPDCT. This type investigation on drug-protein interaction assumes importance in life sciences, chemistry and clinical medicine. Identifying the molecular targets for the beneficial or detrimental effects of small-molecule drugs is an important and currently unmet challenge.

ACKNOWLEDGEMENTS

Financial supports funded by the Shanxi Key Laboratory of Innovative Drug for the Treatment of Serious Diseases Basing on the Chronic Inflammation（Shanxi University of Chinese Medicine, the Fund for Shanxi Key Subjects Construction (FSKSC), the Fund for Shanxi Key Subjects Construction, the Top Science and Technology Innovation Teams of Higher Learning Institutions of Shanxi Province, the Program for the Top Young and Middle-aged Innovative Talents of Higher Learning Institutions of Shanxi Province (2015), Foundation of Young Academic Leader in Shanxi Province, Medicine of Shanxi Province comprehensive development and utilization of collaborative innovation center (2017-JYXT-18) are gratefully acknowledged.

REFERENCES

[1] Chaoqun Y, Jiali Zhang, Taigang Liang, Qingshan Li. Diorganotin(IV) complexes with 4-nitro-N-phthaloyl-glycine: Synthesis, characterization, antitumor activity and DNA- binding studies. *Biomed Pharmacother*. 2015, 71, 119-127.

[2] Y. Li, Z. Wang, P. Guo, L. Tang, R. Ge, S. Ban, Q. Chai, L. Niu, Q. Li. Diorganotin (IV) derivatives of substituted N-hydroxybenzamides with selective cytotoxicity in vitro and potent antitumor activity in vivo. *Inorg Biochem*. 2014, 133, 1–7.

[3] Y. Wei, L. Niu, X. Liu, H. Zhou, H. Dong, D. Kong, Y. Li1, Q. Li. Spectroscopic Studies and Molecular Docking on the Interaction of Organotin Antitumor Compound Bis[2,4-difluoro-N-(hydroxy-<κ>O)benzamidato-<κ>O] diphenyltin(IV) with Human Cytochrome P450 3A4 Protease[J]. *Spectroc. Acta Part A: Molec. and Biomolecular Spec.*, 2016, 163, 154-161.

[4] S. Shityakov, I. Puskas, N. Roewer, C. Forster, J. Broscheit. Three-dimensional quantitative structure- activity relationship and docking studies in a series of anthocyanin derivatives as cytochrome P450 3A4 inhibitors. *Adv Appl Bioinform Chem*. 2014, 7, 11-21.

[5] Y. Zhang, Y. Li, Q. Li. Inhibition of Cytochrome P450 3A in Rat Liver by the Diorganotin (IV) Compound di-n-Butyl-di-(4-chlorobenzo-hydroxamato)tin (IV) and Its Probable Mechanism. Molecules. 2012, 17, 10994-11009.

[6] Yunlan Li,Yang Li,Xiaoqiang Niu,Linjin Jie, Xianmei Shang, Jianping Guo, Qingshan Li. Synthesis and antitumor activity of a new mixed-ligand complex di-n-butyl-(4-Journal of Ichlorobenzohydroxamato) tin(IV) chloride. *Inorg Biochem* 2008, **102**, 1731-1735.

[7] Yunlan Li, Pu Guo, Niu Lin, Qingshan Li. Pharmacokinetics of di-phenyl-di-(2,4-dichlor-benzohydroxamato) tin(IV): A new metal-based candidate with promising antitumor activity in rats. *Inorgan. Chimica Acta.* 2014, **423**, 235-241.

[8] B. Geng, X. Liu, Y. Tian, J. Ye, H. Li, J. Wu. Investigation on the interaction between endocrine disruptor triphenyltin with human serum albumin. *Spectrochim Acta A Mol Biomol Spectrosc.* 2014, **120**, 512-516.

[9] N. Shahabadi, S. Hadidi. Molecular modeling and spectroscopic studies on the interaction of the chiral drug venlafaxine hydrochloride with bovine serum albumin. *Spectrochim Acta A Mol Biomol Spectrosc.* 2014, **122**, 100-106.

[10] R. Revathi, A. Rameshkumar,T. Sivasudha. Spectroscopic investigations on the interacions of AgTiO2 nanoparticles with lysozyme and its influence on the binding of lysozyme with drug molecule. *Spectrochim Acta A Mol Biomol Spectrosc.* **152** 2016, 192-198.

[11] P. Kalaivani, R. Prabhakaran, F. Dallemer.E. Vaishnavi, P. Poornima, V. Vijaya Padma, R. Renganathan, K. Natarajan.Synthesis, structuaral characterization, DNA/Protein binding and in vitro cytotoxicity of isomeric ruthenium carbonyl complexes. *Organomet Chem*.2014, **762**, 67-80.

[12] Anil K. Singh, Abera Asefa. A fluorescence study of differently substituted 3-styrylindoles and their interaction with bovine serum albumin. *Luminescence*. 2009, **24**, 123-130.

[13] Abdulilah Dawoud. Bani-Yaseen. Spectrofluo-rimetric study on the interacion between antimicrobial drug sulfamethazine and bovine serum albumin. *Lumin*. 2011, **131**, 1042-1047.

[14] S. Bi, T. Zhao, H. Zhou, Y. Wang, Z. Li.Probing the interactions of bromchlorbuterol-HCl and phenylethanolamine A with HSA by multi-spectroscopic and molecular docking technique. *Chem. Thermodynamics*, 2016, **97**, 113-121.

[15] A. Hao, X. Guo, Q. Wu, Y. Sun, C. Cong, W. Liu. Exploring the interactions between polyethyleneimine modified fluorescent carbon dots and bovine serum albumin by spectroscopic methods. *Luminscence*, 2016, **170**, 90-96.

[16] Gongke Wang, Ye Chen, Changling Yan, Yan Lu. Study on the interaction between gold nanoparticles and papain by spectroscopic methods. *J. of Luminescence,* 2015, **157**, 229-234.

[17] Swarup Roy, Tapan Kumar Das. Interactions of biosynthesized gold nanoparticles with BSA and CTDNA:A multi-spectroscopic approach. Polyhedron, 2016, **115**, 111-118.

[18] Z. Sun, H. Xu, Y. Cao, F. Wang, W. Mi. Elucidating the interaction of propofol and serum albumin by spectroscopic and docking methods. *Molecular Liquids,* 2016, **219**, 405-410.

[19] M. Kumari, J. K. Maurya, M. Tasleem, P. Singh, R. Patel. Probing HSA-ionic liquid interactions by spectroscopic and molecular docking methods. *Photochemistry and photobiologyB: Biology,* 2014, **138**, 27-35.

[20] Suman Das, Sultana Parveen, Ankur Bikash Pradhan. An insight into the interaction of phenanthridine dyes with polyriboadenylic acid: Spectroscopic and thermodynamic approach. *Spectrochimica Acta Part A: Molecular and Biomolecular Spectroscopy,* 2013, **138**, 356-366.

[21] M. Poór, G. Matisz, S. Kunsági-Máté, D. Derdák, L. Szente, B. Lemli. Fluorescence spectroscopic investigation of the interaction of citrinin with native andchemically modified cyclodextrins. *J. of Lumin.*, 2016, **172**, 23-28.

[22] P. Fan, Lu Wan, Y. Shang, J. Wang, Y. Liu, X. Sun, C. Chen. Spectroscopic investigation of the interaction of water-soluble azocalix [4] arenes with bovine serum albumin. *Bioorganic Chemistry*, 2015, **58**, 88-95.

[23] T. Hu, Y. Liu. Probing the interaction of cefodizime with human serum albuminusing multi-spectroscopic and molecular docking techniques. *J. of Pharm. & Biom. Analysis,* 2015, **107**, 325-332.

[24] L. Lai, C. Lin, Z. Xu, X. Han, F. Tian, P. Mei, D. Li, Y. GeX, F. Jiang, Y. Zhang, Y. Liu. Spectroscopic studies on the interactions between CdTe quantum dots coated with different ligands and human serum albumin. *Spectroc. Acta Part A: Molec. & Biom. Spec.*, 2012, **97**, 366–376.

[25] L. Tian, X. Hu, Z. Liu, S. Liu. Studies on the interaction of heparin with lysozyme by multi-spectroscopic techniques and atomic force microscopy. *Spectroc. Acta Part A: Molecular & Biomolecular Spectroscopy,* 2016, **154**, 27-32.

[26] Q. Wang, C. Huang, M. Jiang, Y. Zhu, J. Wang, J. Chen, J. Shi. Binding interaction of atorvastatin with bovine serum albumin: Spectroscopic methods and molecular docking. *Spectrochimica Acta Part A: Molecular and Biomolecular Spectroscopy*, 2015, **156**, 155–163.

[27] V. D. Suryawanshi, Laxman S. Walekar, A. H. Gore, P. V. Anbhule. Spectroscopic ananlysis on the binding interaction of biolioically active pyrimidine detrvative with bovine serum albumin. *Pharm. Analysis,* 2016, **6**, 56-63.